3rd EUROPEAN CONFERENCE ON
EARTHQUAKE ENGINEERING & SEISMOLOGY
BUCHAREST, ROMANIA, 2022

Full-scale shake table tests of a reinforced concrete structure equipped with a novel active mass damper

Paolo M. Calvi – University of Washington, Seattle, USA, e-mail: pmc85@uw.edu

Giovanni Rebecchi – ISAAC antisismica, Milano, Italy, e-mail: giovanni.rebecchi@isaacsrl.com

Matteo Rosti – ISAAC antisismica, Milano, Italy, e-mail: matteo.rosti@isaacsrl.com

Alberto Bussini – ISAAC antisismica, Milano, Italy, e-mail: alberto.bussini@isaacsrl.com

Stefano Cii – ISAAC antisismica, Milano, Italy, e-mail: stefano.cii@isaacsrl.com

Davide Bolognini – Eucentre, Pavia, Italy, e-mail: davide.bolognini@eucentre.it

Filippo Dacarro – Eucentre, Pavia, Italy, e-mail: filippo.dacarro@eucentre.it

Luca Grottoli – Eucentre, Pavia, Italy, e-mail: luca.grottoli@eucentre.it

Francesco Ripamonti – Politecnico di Milano, Italy, e-mail: francesco.ripamonti@polimi.it

Abstract: This paper presents the results of an experimental program involving shake table testing of two full-scale reinforced concrete frame buildings. These tests were conducted to investigate the effectiveness and reliability of a newly proposed servo-hydraulic Active Mass Damper (AMD) that can be designed to enhance the target seismic performance of a building at multiple earthquake intensity levels.

The two nominally identical case-study buildings were intentionally designed to exhibit a "soft story" mechanism at the first level when subject to ground shaking of sufficient intensity, but one was equipped with the newly proposed AMD, installed on the roof. The two specimens were then subject to the same loading protocol consisting of a ground shaking sequence of varying intensity, with the seismic input consisting of a selected natural ground motion.

The experimental results demonstrated that the proposed AMD is extremely effective at enhancing building seismic performance. Specifically, the AMD provided peak displacement reductions in the order of 70% and was shown capable of absorbing more than 60% of the total input energy. As a consequence, the un-retrofitted structure suffered nontrivial structural and non-structural damage, while the AMD-retrofitted building remained virtually undamaged at all shaking intensities considered.

Keywords: active mass damper; full-scale shake table; reinforced-concrete buildings; enhancing seismic performance; tuned-mass damper.

1. Introduction

A novel servo-controlled Active Mass Damper (AMD) for the protection of structures against the effects of earthquakes was recently proposed in Rebecchi et al. (2022) A prototype is shown in Fig. 1. It consists of an innovative inertial system used as Active Vibration Control device that, differently from other AMDs, uses an electro-hydraulic actuator to move the inertial mass. The design, fabrication and preliminary testing of the prototype AMD has been carried out at the Politecnico di Milano, Italy. A brief description of the system is provided herein, while more details can be found in the companion paper by Rosti et al. (2022). For a more comprehensive discussion on active mass dampers, interested readers can refer to De Roek (2011), Dyke et al. (1996), Forrai et al. (2001), Moutinho et al. (2011), Chu et al. (2005), Saito et al. (2001), Xu et al. (2014), Connor and Laflamme (2014), Yamamoto and Sone (2014), Nakamura et al. (2001).

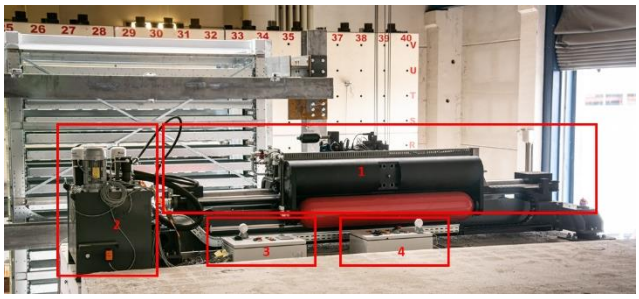

Fig. 1 - The AMD proposed: 1) hydraulic cylinder; 2) oil restoration control unit; 3) control panel and fault management; 4) control panel and fault management of hydraulic control unit

The AMD prototype is made up of a fixed part which transmits the force to the floor of the building it is connected to, and a moving part which is responsible for generating the control force. The latter has a weight of 2200 kg, while the overall weight of the system is 4000 kg. The plan dimensions of the device are 4.8 m by 1.5 m, the height is 1.3 m.

The purpose of the AMD is to generate inertial forces that "counteract" the movement of the building by reducing the amplitude of oscillation and, consequently, the earthquake-induced forces experienced by the structural elements. The magnitude of the inertial forces to be generated is calculated in real time by the control algorithm, based on the accelerometric readings of sensors installed at certain locations across the structure.

Ideally, the AMD is to be installed on the roof of a building, with one or more devices acting in at least two orthogonal directions to reach the desired three-dimensional performance (optimal arrangement is determined on a case-by-case basis). It is also possible to install the AMDs at lower levels, if compatible with architectural and construction constraints.

The AMD comprises four main subsystems: sensors, controller, actuators and power system. The sensors are elements which provide the feedback needed for the control. They are installed on the structure to measure system response variables, such as displacements, velocities and accelerations. The sensors can also be used to perform tasks such as structural health monitoring, by allowing the dynamic identification of the structure during its life cycle. The controller is the core of the AMD because it implements the vibrating control algorithm. It produces actuation signals by a feedback function of sensor measurements and defines the inertial mass displacement in time. Many types of control exist in the literature. The “Sky-Hook”, a direct velocity feedback control which does not need the creation of a building model, was chosen for its performance and robustness. The algorithm defines a control force proportional to the relative velocity of the building and this force is produced by the double acting hydraulic actuator used to move the inertial mass. The actuator can generate a linear force up to 220 kN, with maximum velocity and displacement amplitude of 5 m/s and ±0.5m, respectively.

The AMD has been tested and tuned via Hardware-In-the-Loop (HIL) simulations over the course of previous studies. In these hybrid analyses the AMD prototype was coupled with numerical models of case study buildings, to assess its behavior in real-time. These tests were used to study the response of the AMD and its effects on the structure at different earthquake intensities. Due to the limitations of the HIL test rig, earthquake inputs with a maximum PGA of 0.15g were simulated. Promising results were obtained, including reductions in roof displacements and accelerations of about 70% and 50%, respectively. During all tests, the AMD displayed excellent behavior, tracking with high accuracy the reference force to be generated.

The study presented in this paper investigated the performance of the newly proposed AMD under more realistic working conditions, further assessing its capabilities at enhancing the seismic performance of buildings. This was achieved via shake table testing of two nominally identical full-scale reinforced concrete frame structures with masonry infills, one of which equipped with the AMD, installed on the roof. The two specimens were not designed according to any particular design code and were not intended to be representative of any specific building typology or class of buildings. However, they were intentionally designed to exhibit a "soft story" mechanism at the first level when subject to ground shaking of sufficient magnitude. Soft story issues have been observed repeatedly and extensively over the course of past seismic events (e.g., Olive View Hospital during 1971 San Fernando, California earthquake, Bertero et al. (1973)), making the case-study building ideal candidates to demonstrate the effectiveness of the proposed AMD at enhancing the seismic performance of realistic structures affected by a major structural deficiency.

In the sections that follow, the results of the shake table experiments are discussed and used to draw some preliminary conclusions pertaining to the behavior, reliability, and effectiveness of the proposed AMD, and to assess the enhanced seismic performance of AMD-retrofitted RC buildings. More details can be found in Rebecchi et al. (2022).

2. Experimental program and setup

2.1. Description of the specimens

The elevation views of the nominally identical full-scale specimens are shown in Fig. 2a). The two specimens were 3-story one-bay (in both directions) frame buildings, made of RC columns with 20 x 20 cm cross section, connected to 40 cm thick RC slabs. The columns were reinforced with 4 longitudinal 16 mm diameter steel bars in the corners, and 8 mm diameter closed stirrups spaced at 100 mm (Fig. 2b).

The floor plan dimensions were 5.0 x 2.1 m, and the clear inter-story height was 2.5 m. Building A (not equipped the AMD) had a total height of 8.84 m, while Building B was 8.7 m tall. The different building height was due to the increased slab thickness (from 40 cm to 54 cm) at the roof level of Building A (see Fig. 2). This was done to compensate the roof weight added by the AMD in Building B which resulted in a total increase of mass of only the 1%. It should be noted that in case of real structures, the weight added by the AMD system(s) is not expected to exceed 1% of the total weight of the building.

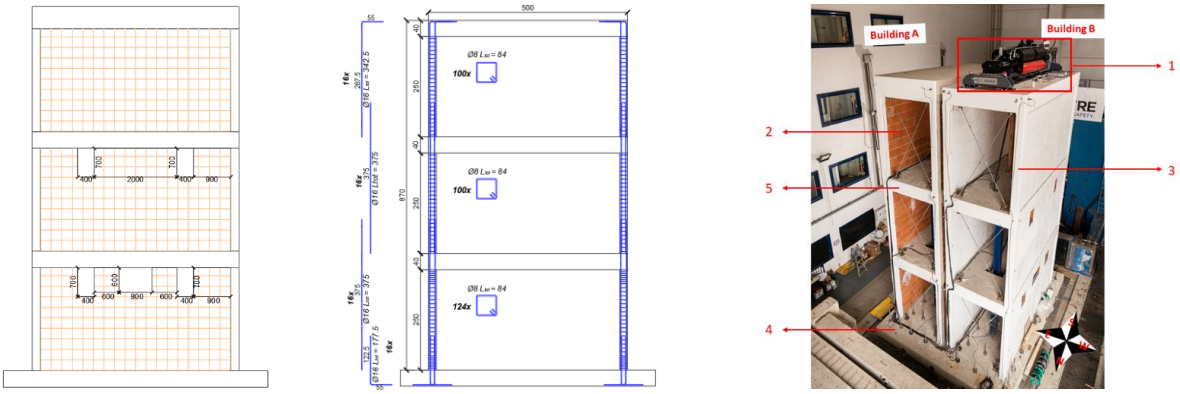

(a) *(b)* *(c)*

Fig. 2 - a) Elevation view of the buildings; b) Reinforcement details of the columns; (c) The buildings tested in the Eucentre laboratory: 1) AMD; 2) masonry infills; 3) columns; 4) foundation slab connected to the shake table; 5) floor slabs.

Infill masonry walls made of 8 x 25 x 25 cm clay blocks were installed in the N-S direction (i.e., the excitation direction) at each floor. The infill walls were coated externally with a layer of plaster and presented a series of openings, as shown in Fig. 2a.

The two specimens were connected to the same foundation slab, which was bolted down to the shake table using post-tensioned steel bars. The distance between the two buildings was about 20 cm. A view of the buildings and AMD control system in their pre-test configuration is shown in Fig. 2c.

The response of both the shake table and the specimens was monitored in real time through an array of instruments including 20 accelerometers, 19 displacement transducers and an optical acquisition.

2.2. Experimental setup and loading protocol

The full-scale specimens described in the previous section were tested on the unidirectional shake table in the Shake-LAB at the Eucentre facility, Italy.

The specimens were tested by applying the E-W component of the Irpinia earthquake, which hit central Campania and central-northern Basilicata on the 23rd of November 1980. The main characteristics of this record are: a) peak ground acceleration PGA = 0.32 g; b) effective duration TD = 6.32 s; c) Arias intensity Ia = 1.41 m/s; d) absolute cumulative velocity CAV = 10.88 m/s. The acceleration history record and acceleration response spectrum for the 100% intensity level are presented in Fig. 3.

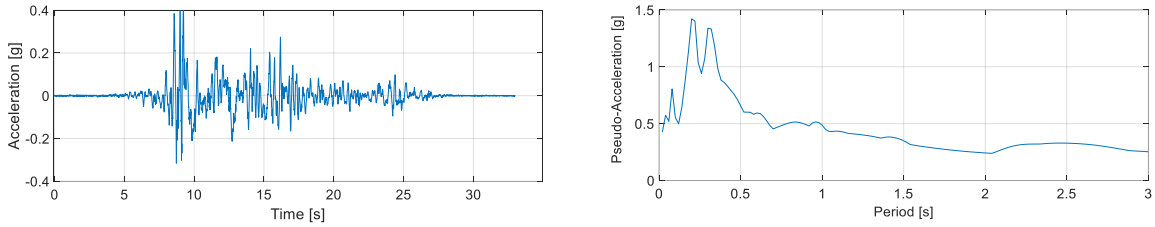

(a) *(b)*

Fig. 3 - a) Acceleration history of the reference record; b) pseudo-acceleration response spectrum at 5% damping

The shake table experiments were conducted in 5 phases, over the course of three days. Each testing phase involved the application of the Irpinia record (i.e., the reference earthquake), considering scale factors ranging from 0.10 to 1.37, for a total of 19 tests, labelled CMP1 to CMP19. More details can be found in Rebecchi et al. (2022).

3. Experimental results

3.1 Damage progression

In this section, the performance of the specimens is assessed as a function of the level of damage detected following each test. The key observations can be summarized as follows:

- For earthquake intensities ranging from 10% to 60% of the reference input ground motion, both buildings exhibited essentially elastic behavior, with only a few small cracks (less 0.5 mm wide) occurring in the corner of infill panel at ground floor;
- For earthquake intensities ranging from 60% to 70% of the reference input ground motion, Building A (uncontrolled) suffered nontrivial widening of the existing cracks and experienced the formation of widespread new cracks in the infill walls of the

ground floor; in contrast, Building B (controlled) only exhibited minor propagation of the pre-existing cracks;

- The 137% earthquake intensity (the largest scale factor considered) induced considerable damage in Building A that included extensive cracking and spalling of the infill walls in the top corner regions of the first floor (Fig. 4a) and structural damage in the form of diagonal cracks in the nodal panels of the slab-column connections. In contrast, Building B remained virtually undamaged (Fig. 4b), only exhibiting negligible widening of some of the cracks formed during previous testing phases.

(a) *(b)*

Fig. 4 - Detailed view of a selected region of the Buildings: a) cracking of the column-slab joint region of the first floor in Building A, b) column-joint region of Building B with no signs of distress.

3.2 Floor displacement and AMD time-history response

The floor displacement/drift results of the shake table tests are presented in this section. Figure 5 shows the peak first floor inter-story drifts for the two specimens during all testing phases. At shaking intensities ranging from 10% to 70% of the reference earthquake (CMP 1 to CMP 11), the maximum first story drift recorded for Building B was consistently 50% to 65% lower than that recorded for Building A. This is evidence that the AMD is beneficial and provides good control of the structural response at low-to-medium intensity shakings (i.e. at "serviceability" conditions).

The benefits of the AMD with respect to limiting the inter-story drift of the critical floor become even more prominent (and somewhat more relevant) in the case of high-intensity input ground motions. During test CMP 19, the first story of Building A reached a peak horizontal displacement of 22.5 mm, corresponding to a 0.90% inter-story drift ratio. For the same seismic input, the peak displacement of the first floor of Building B was only 6.3 mm, equaling an inter-story drift ratio as low as 0.25%. Thus, with the structures subject to high intensity shaking, the AMD induced a drift demand reduction of 72% at the critical level. As discussed in the previous section, this translates into a remarkable reduction of the extent of damage experienced by the building.

It is evident that the inter-story drifts for Building A were critical at the first floor (as per design objectives). However, while not explicitly shown here, they were relatively controlled at levels 2 and 3, with peak ratios recorded during test CMP 19 of 0.32% and 0.14%, respectively. At those same levels, Building B reached peak drift ratios of 0.18% (at both floors), thus exhibiting a uniform building response, with well-controlled drift values across the height. This is an excellent outcome as it confirms that the AMD successfully addressed the existing structural deficiency at the first floor, without compromising the structural response at other levels.

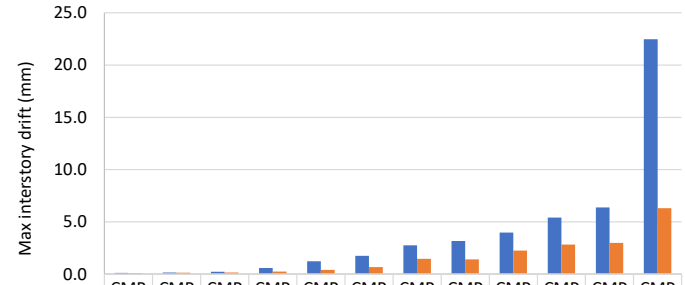

	CMP 1	CMP 2	CMP 3	CMP 4	CMP 5	CMP 6	CMP 7	CMP 8	CMP 9	CMP 10	CMP 11	CMP 19
Building A	0.1	0.1	0.2	0.6	1.2	1.7	2.7	3.2	4.0	5.4	6.4	22.5
Building B	0.1	0.1	0.1	0.2	0.4	0.7	1.5	1.4	2.3	2.8	3.0	6.3

Fig. 5 - Graphical and numerical representation of the maximum interstory drift recorded at the first floor of both buildings during each test.

Fig. 6 (left) shows the first floor inter-story drift for both Buildings A and B. All of Building A's peak drifts exceeding 20 mm are identified on the graph and marked with blue asterisks. The corresponding peak drift values recorded for Building B are marked with red circles. Note that there is a slight time misalignment between the peak displacements experienced by the two buildings (due to the different response of the two structures), but this offset never exceeds 0.5 s.

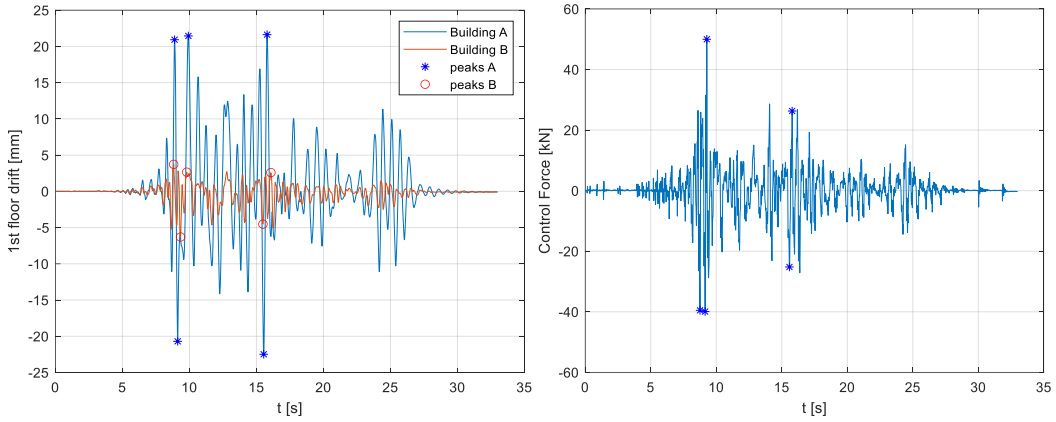

Fig. 6 - First floor inter-story drift for both buildings (left) and AMD control force (right) during test (CMP 19)

It can be seen that the five largest peak drifts of Building B are, on average, about 18% of those recorded for Building A (3.94 mm against 21.42 mm). It is clear that this remarkable drift reduction is to be attributed to the contribution provided by the AMD. To emphasize this aspect, the AMD control force time history is provided in Fig. 6 (right). The five force values corresponding to the peak displacements outlined in Fig. 6 (left) are identified and marked. It can be seen that large forces with opposite sign with respect to the 1st floor inter-story drift detected for Building A are generated, that effectively counteract the movement of the building by reducing the amplitude of oscillation.

These results demonstrate that the performance of the case study building was significantly enhanced by the presence of the AMD, in terms of inter-story drifts and overall damage to structural and non-structural elements. The two main aspects that contribute to enhancing the building seismic performance are the inertial force generated and the amount of input energy absorbed by the AMD.

The maximum displacement of the mobile mass relative to the roof recorded during the strongest shaking was 116.7 mm, while the maximum inertial force generated by the AMD

was approximately 51 kN. The AMD displacement and force limits are 500 mm and 220 kN, respectively. Thus, enhancing the performance of the case-study building tested in this study required the AMD to reach only 23% of its peak capacity.

The energy absorbed (comprehensive of the kinetic energy) by the various components of the structures is shown in Fig. 7. Several observations can be made from the available data. For instance, the input energy for Building B is about 32% higher than for Building A (16.2 kJ and 12.6 kJ, respectively). However, the AMD dissipated roughly 63% of the total input energy, with the structure absorbing the remaining 37%. This corresponds to only 6.1 kJ, against the 12.6 kJ energy absorbed the structure of Building A. Thus, the energy dissipated solely by the structure in the AMD-equipped system was only 50% of the energy absorbed by the un-retrofitted building.

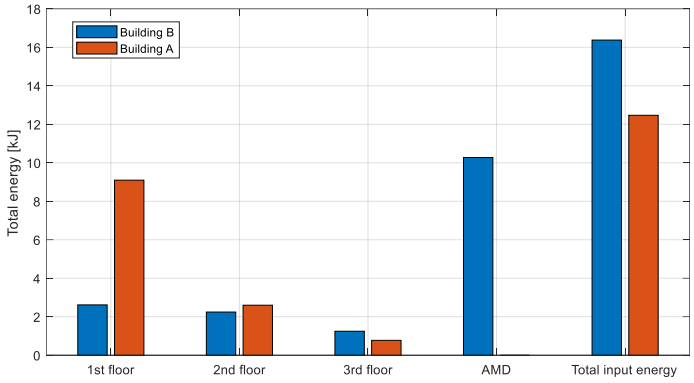

Fig. 7 - Energy balance in both buildings (test CMP 19).

Evidently, the lower the amount of energy to be absorbed, the lower the extent of damage to structural and non-structural elements. It is also interesting to notice that in the un-retrofitted case (Building A), about 71% of the total input energy was absorbed by the first floor. This is consistent with the results presented in the previous sections, and with the notion that the most severe seismic demand occurs at the first story that exhibited the greatest extent of damage and experienced the highest horizontal displacements. However, a much different trend is seen for Building B. By virtue of the AMD, there is a clear and favorable energy absorption shift whereby the amount of energy affecting the first floor is reduced to only 15% of the total input energy. This value is much closer to that observed for the second and third floors, indicating a much more uniform structural response. The reduction obtained on energy absorption of the overall structure is slightly more than 50%, but this percentage raises up to a 71% reduction on the first floor elements that are the most critical elements during a seismic event.

4 Conclusion

Full-scale shake table tests were conducted to investigate the effectiveness of a newly proposed AMD, at protecting structurally deficient RC buildings from the effects of earthquakes. The operating principles of the tested AMD are based on the feedback received by sensors installed at strategic locations across the building. These measurements are processed by a central computer and the data elaborated via a control algorithm allow the actuator to move the inertial mass on the building roof. A control force is generated in real time that counterbalances the forces of inertia induced by the earthquake.

The AMD was installed on the roof of one of two nominally identical full-scale RC frame building specimens, intentionally designed to exhibit a “soft story” mechanism at the first level. The buildings were tested on the unidirectional shake table available in the Shake-LAB at the Eucentre facility (Italy), under a real ground motion of increasing intensity.

The experimental results showed that the un-retrofitted building (i.e., the building not equipped with the AMD) suffered significant structural and non-structural damage, particularly at the first floor of the building. In contrast, the AMD-retrofitted structure remained virtually undamaged even after being subject to the strongest shaking considered. It was shown that the AMD absorbed about two thirds of the total input energy, and provided excellent building protection, substantially reducing floor displacements and leading to a significantly more uniform building response. Most notably, the AMD induced a 72% reduction of the peak inter-story drift recorded at the critical level, effectively addressing the main structural deficiency that affected the case-study buildings. This reduction of the peak inter-story drift is consistent with the results of the energy balance that highlight a 71% reduction of energy absorbed by the elements of the first floor in the AMD-retrofitted building.

Acknowledgements

This experimental program described in this paper is part of a research project led and funded by ISAAC antisismica and 360 Capital Partners, with the aim of promoting the use of Active Mass Dampers to enhance the seismic performance of new and existing buildings.

References

- Bertero V. V., Bresler B., Selna L.G., Chopra A.K. , Koretsky A.V. (1973). Design implications of damage observed in the Olive view medical center buildings. Proceedings of the 5 th World Conference on Earthquake Engineering.
- Chu S., Soong T., Reinhorn A. (2005). Active Hybrid and Semi-Active Structural Control, John Wiley and Sons, Ltd, England. ISBN: 978-0-470-01352-6.
- Connor J., Laflamme S. (2014). Structural Motion Engineering, Springer International Publishing. ISBN: 978-3-319-06281-5.
- De Roeck G. (2011). A versatile active mass damper for structural vibration control. Proceedings of the 8th International Conference on Structural Dynamics. Leuven. 1777–1784.
- Dyke S., Spencer B., Quast P., Kaspari Jr. D., Sain M. (1996) Implementation of an active mass driver using acceleration feedback control, Microcomput. Civil Eng. 11:305–323.
- Forrai A., Hashimoto S., Isojima A., Funato H., Kamiyama K. (2001). Gray box identification of flexible structures: application to robust active vibration suppression control, Earthquake Engineering Structural Dynamics. 30:1203–1220.
- Moutinho C., Cunha A., Caetano E. (2011). Implementation of an active mass driver for increasing damping ratios of the laboratorial model of a building, Journal of Theoretical and Applied Mechanics. 49:791–806.
- Nakamura Y., Tanaka K., Nakayama M., Fujita T. (2001). Hybrid mass dampers using two types of electric servomotors: AC servomotors and linear-induction servomotors, Earthquake Engineering Structural Dynamics. 30:1719–1743.
- Rebecchi G., Calvi P. M., Bussini A., Dacarro F., Bolognini D., Grottoli L., Rosti M., Ripamonti F., Cii S. (2022). Full-scale shake table tests of a reinforced concrete building equipped with a novel servo-hydraulic active mass damper, Journal of Earthquake Engineering, under review.
- Rosti M., Cii S., Bussini A., Ripamonti F., Calvi P.M. (2022). Design and Validation of a Hardware-In-the-Loop Test Bench for the Performance Evaluation of an Active Mass Damper, Journal of Vibration and Control, under review.
- Saito T., Shiba K., Tamura K. (2001). Vibration control characteristics of a hybrid mass damper system installed in tall buildings, Earthquake Engineering Structural Dynamics. 30:1677–1696.
- Xu H.B., Zhang C.W., Li H., Ou J. P. (2014). Real-time hybrid simulation approach for performance validation of structural active control systems: a linear motor actuator based active mass driver case study, Structural Control Health Monitoring. 21:574–589.
- Xu H.B., Zhang C.W., Li H., Tan P., Ou J.P., Zhou F.L. (2014). Active mass driver control system for suppressing wind-induced vibration of the canton tower. Smart Structures and Systems. 13:281–303.
- Yamamoto M., Sone T. (2014). Behavior of active mass damper (AMD) installed in high-rise building during 2011 earthquake off pacific coast of Tohokuand verification of regenerating system of AMD based on monitoring. Structural Control Health Monitoring. 21:634–647.